IJE TRANSACTIONS C: Aspects Vol. 28, No. 9, (September 2015) 1383-1391

International Journal of Engineering

Journal Homepage: www.ije.ir

Investigation on Tensile Strength of Friction Stir Welded Joints in PP/EPDM/Clay Nanocomposites

G. R. Rezaei, N. Bani Mostafa Arab*

Faculty of Mechanical Engineering, Shahid Rajaee Teacher Training University, Tehran, Iran

PAPER INFO

Paper history:
Received 25 May 2015
Received in revised form 12 July 2015
Accepted 30 July 2015

Keywords:
Nanocomposite
Friction Stir Welding
Clay
Response Surface Method
Tensile Strength

ABSTRACT

Polymer-based nanocomposites due to good corrosion resistance, adequate mechanical properties and low cost are widely used in modern technologies. Because of the increasing application of these nanocomposites, their joining through welding processes seems unavoidable. In this paper, 5mm thick nanocomposite plates containing polypropylene, ethylene-propylene diene monomer with 0, 3 and 6% clay were butt welded using a novel hot tool in friction stir welding process. Response surface method is used to design experiments and determine the effect of process parameters such as tool rotational speed, welding speed, tool shoulder temperature and clay content on weld tensile strength. The results show that although increasing clay content in the base material increases its tensile strength, but decreases the tensile strength of the weld such that in specimens with 0, 3 and 6% clay content, the tensile strength of the weld equals 94, 80 and 61 percent of the respective base materials.

doi: *10.5829/idosi.ije.2015.28.09c.17*

1. INTRODUCTION

In recent years, developing materials with enhanced strength to weight ratio and toughness as well as low cost such as polymer-based nanocomposites is gaining attention in industries such as transportation [1-3]. The addition of very small amounts of nanoparticles (less than 10% of weight) as the reinforcing material to polymers is used to improve their mechanical and thermal properties. Nanocomposites are composed of two phases. The first phase is the base or matrix of the nanocomposite and can be made up of a polymer, metal, or ceramic, and the second phase or reinforcement phase, includes nanoparticles, nanosheets, nanofibers and nanotubes. Nanoparticles are widely utilized in nanocomposites as the reinforcing material [2, 4]. Nanoclay is the nanoparticle that is often used in fabrication of nano-composites [5].

Nowadays a lot of attention is paid to joining of thermoplastic nanocomposites in different industries because it is widely employed instead of metals and their alloys. One way to join nanocomposites is through welding. Among welding processes, friction stir welding (FSW) which is a solid-state joining process can be a candidate for joining these materials. In this process, a non-consumable tool with a specially designed pin and shoulder is inserted into the sheets or plates to be joined and traversed along the joint line. FSW is based on heat supplied by the friction between a rotating tool and the parts to be welded which causes plastic deformation and stirring of the parts at the joint area [6-8]. The review of previous works shows that when conventional FSW is applied to polymer and composite materials, it is very difficult to achieve high quality welds due to low melting temperature and low thermal conductivity of these materials [9-11]. Research done by Yosefpour et al. indicates that FSW is a suitable method for welding thermoplastic composites [12]. Zoltan Kiss et al. [13] used FSW for polypropylene (PP) sheets and investigated the effect of parameters such as rotational speed, linear speed and tool geometry on the bond strength. They concluded that the tool geometry had a stronger effect than the

*Corresponding Author's Email: n.arab@srttu.edu (N. Bani Mostafa Arab)

Please cite this article as: G. R. Rezaei and N. Bani Mostafa Arab, Investigation on Tensile Strength of Friction Stir Welded Joints in PP/EPDM/Clay Nanocomposites, International Journal of Engineering (IJE), TRANSACTIONS C: Aspects Vol. 28, No. 9, (September 2015) 1383-1391

other two parameters on bond strength. Payeganeh et al. [14] investigated the effect of pin geometry and FSW process parameters on mechanical properties of pp composite welds. Their results indicated that pin geometry had a significant effect on weld surface appearance and weld tensile strength. Pirizadeh et al. [15] used a new tool named ''self-reacting tool'' to weld acrylonitrile butadiene styrene (ABS) sheets. They studied the effect of shape of the pin, rotational speed and transverse speed on mechanical properties. Their results show that pin shape has the greatest effect on tensile strength of welded parts. Azarsa et al. [16] investigated the effect of critical process parameters such as rotational speed, shoe temperature and traverse speed on the flexural strength of friction stir welded joints of the high density polyethylene (HDPE). They concluded that welding at a lower level of tool travel speed and a high level of rotational speed increased weld flexural strength by reducing size of defects. Mendes et al. [17] studied the influence of axial force, tool rotational and traverse speed on quality of ABS plates. Their results show that high rotational speed and high axial force are required to produce welds free of defects. The past works show that there are no reported publications concerning modeling and optimization of process parameters in FSW of nanocomposites. In this work, an experiment is therefore designed using Box–Behenken design and a new hot tool to study the effect of rotational speed, welding speed, shoulder temperature and clay content on the weld strength of PP / ethylene-propylene diene monomer (EPDM) / Clay nanocomposite. The MINITAB software is used to create the design matrix and analyze the experimental data [18].

2. EXPERIMENTAL PROCEDURE

2. 1. Materials Polypropylene (Z30s) with a density of 0.9 g/cm^3 and melt flow index of 25 g/10 min, EPDM Keltan 3072 (Mooney viscosity ML (1+8 min) 120°C = 48 M, 64% ethylene and 8.7% ENB content) and the organoclayCloisite® 15A with a specific gravity of 1.66 were the materials used in this study.

2. 2. Sample Preparation The blend PP/EPDM and PP/EPDM/clay nano-composite with 3 and 6 %wt clay content were formed by melt compounding in a BrabenderPlas-Corder twin screw extruder (length = 1000 mm, L/D = 40) and co counter-rotating type with the barrel temperature profile of 160, 165, 175, 185 and 190° C from the hopper to die, feeding rate of 1 kg/h and screw speed of 150 rpm. Test specimens with 200×200×5 mm dimension were prepared using Collin P 200 E-type hot press.

2. 3. Test procedures

2. 3. 1. X-ray Diffraction X-ray diffractometer (XRD) was used to evaluate the dispersion of the clay in the polymer matrix. XRD experiments were carried out with a Philips -X'Pert diffractometer at room temperature in the low angle of 2θ. The X-ray beam was a CuKα radiation (λ = 1.540598 A) operated at 50 kV voltage and 40 mA current. The 2 mm thick test specimens for XRD were prepared by compression molding. The scanning rate was 0.5°/min and the experiments were performed in the angle range of 0-10.

2. 3. 2. Tensile Test Procedure The tensile properties of the samples were determined according to standard ASTM D638. Tensile tests were carried out at 23°C with a cross-head speed of 50 mm/min using the Zuker tensile test machine. Table 1 shows the weight percent composition and tensile strength of the base materials.

2. 3. 3. FSW Tool and Equipment A FP4M milling machine was used for butt welding the two specimens of 100×50×5 mm size. A newly designed FSW tool consisting of a cylindrical shoulder made of AA7075 aluminum alloy with two electric heaters placed in the shoulder with a taper grooved pin made of H13 hot – working steel was used. A ball bearing separated the fixed hot shoe from the pin during welding. Rotational velocity (ω), linear velocity (V), shoulder temperature (T) were considered as the input process parameters. A number of trial runs were performed in order to determine the working limits of the process parameters. Figures 1 and 2 show low quality welds with process parameters set outside the working limits. The input parameters levels and their coded and actual values used in the experimental design matrix are presented in Table 2.

TABLE 1. Properties of the base materials

Sample	Weight percent	Failure force (N)	Maximum stress (MPa)
PP/EPDM	PP, EPDM: 80, 20%	53.55	15.3
PP/EPDM/Nanoclay	PP, EPDM, Nanoclay: 77, 20, 3%	59.85	17.1
PP/EPDM/Nanoclay	PP, EPDM, Nanoclay: 74, 20, 6%	73.5	21

TABLE 2. The input parameters

Parameter	Unit	Symbol	Levels		
			-1	0	1
Clay nanoparticles	%	C	0	3	6
Rotational velocity	rev/min	ω	800	1200	1600
Linear velocity	mm/min	V	10	15	20
Temperature	℃	T	50	75	100

Figure 1. Low quality welds at (a) high rotational speed (b) low rotational speed

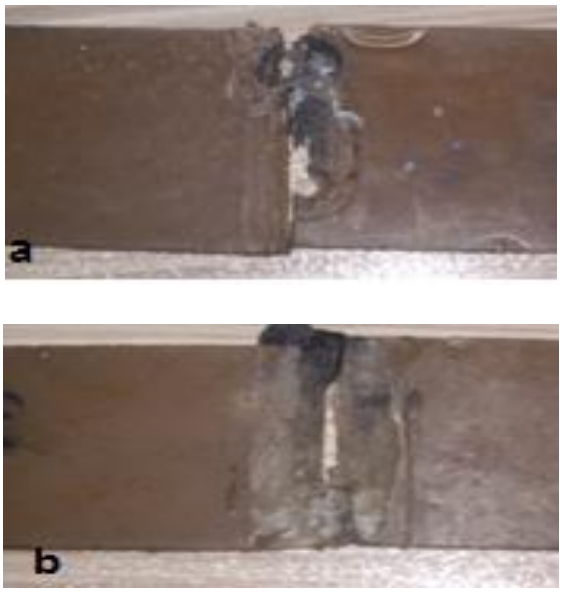

Figure 2. Low quality welds at (a) high welding speed (b) low welding speed

2. 3. 4. Scanning Electron Microscopy The fracture surfaces of the weld samples were coated with gold and examined by a JXA-840 scanning electron microscope (SEM) with an operating voltage of 20 KV.

3. RESULTS AND DISCUSSION

3. 1. XRD Analysis The XRD diffraction pattern of PP/EPDM/clay nanocomposites is shown in Figure 3. The d-spacing of clay and nanocomposites was obtained from Bragg's law, $d= \lambda/ (2\sin\theta)$. According to literature reviews, diffraction peak related to the basal spacing (d001) of neat clay appears at 2.9° (corresponding d-spacing is 30.44 Å), while the diffraction peaks and the interlayer distance of nanocomposite with 6 and 3 % nanoclay are shifted to lower angles of 2.81° (31.52 Å) and 2.36° (34.89 Å), respectively. The lower diffraction angle of nanocomposite in comparison with that of the clay shows polymer chains can intercalate between the layers of the clay.

3. 2. Analysis of Variance The response surface methodology (RSM) was applied to data using the MINITAB 16 software to create the design matrix. 27 sets of actual conditions were used for welding and the averages of three measured responses (tensile strength) were used for analysis which is shown in appendix A. Analysis of the tensile strength (response) was done by the above software. Analysis of variance (ANOVA) for the response is presented in appendix B. A model or model term is significant when its p-value is less than 0.05. Analysis of variance, lack of fit and F-test were used to check the adequacy of the model and determine the significant model and model terms. From appendix B, it is observed that the linear and quadratic effects of clay content (C), rotational speed (ω), travel speed (V) and shoulder temperature (T) are significant.

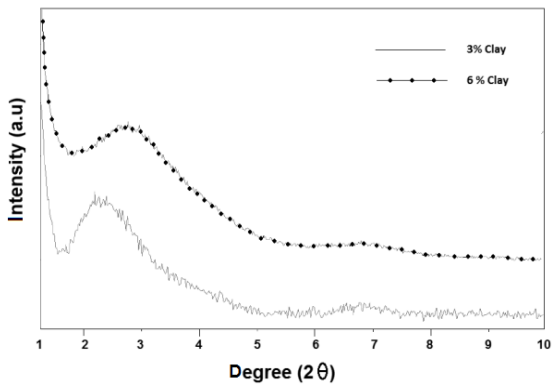

Figure 3. XRD patterns of PP/EPDM/clay nanocomposites

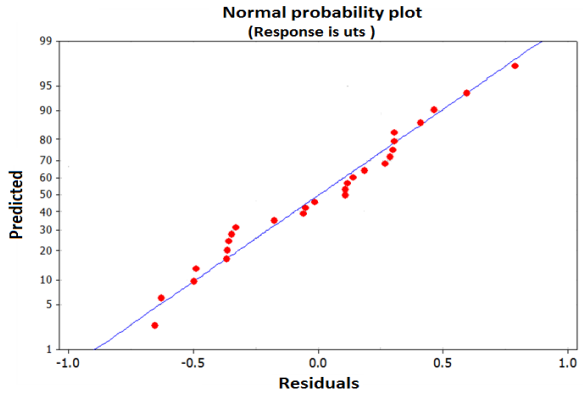

Figure 4. Normal distribution diagram of the model

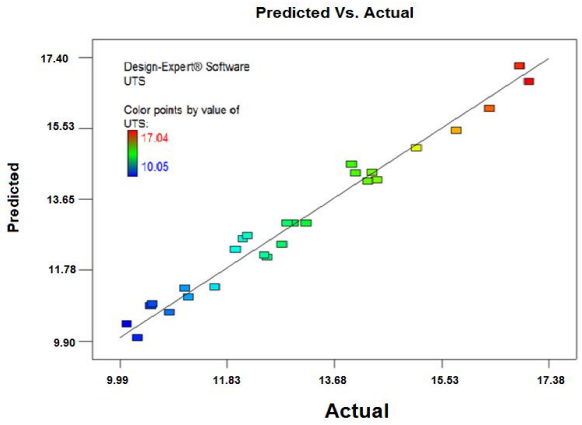

Figure 5. Predicted versus actual values of the weld strength

The interaction effects of rotational speed and travel speed (ω×V), travel speed and shoulder temperature (V×T) are also significant. The adj. R^2 value of 0.9209 and the R^2 value of 0.9635 are high and close to 1 which is an indication of an adequate model. Figure 4 shows the normal probability plot of the residuals which is another tool for checking the adequacy of the model. Since the points on the normal probability plot of the residuals form a straight line, it can be concluded that the model is adequate. Based on this analysis, the final mathematical model for estimation of the tensile strength within the design space, is given in terms of coded and actual factors in Equations (1) and (2), respectively.

(a) In terms of coded factors

$$UTS= 10.02 – 1.31\ C + 1.63\ – 1.01\ V + 0.539\ T + 0.57\ C*C + 0.79\ \omega*\omega – 0.593\ V*V – 0.764\ T * T – 1.53*\omega*V – 1.21*V*T \quad (1)$$

(b) In terms of actual factors

$$UTS= -18.07 – 2.55\ C + 0.0038\ \omega + 2.03\ V + 0.354\ T + 0.063\ C*C + 0.0000049\ \omega*\omega – 0.023\ V*V – 0.0012\ T * T – 0.00076\ \omega*V– 0.0096*V*T \quad (2)$$

3. 3. Validation of the Mathematical Model

Checking the validity of the developed model was performed by three seperate tests. These tests were performed under conditions diffrent from the other 27 tests in the research. The actual results, predicted values and calculated percentage errors are presented in Table 3. It can be seen that the error value is smaller than 6%, which indicates that the mathematical model for prediction of weld strength is acceptable within the limits of the parameters. Figure 5 shows the plot of the actual and predicted values of the weld strength. This figure also shows that the model is adequate and there is a good agreement between the experimental and predicted results.

3. 4. Effect of Process Parameters on the Response

3. 4. 1. The Effect of Clay Content on Tensile Strength Figure 6 shows the effect of clay content on tensile strength of the welds. It indicates that with increasing clay content from 0 to 3%, the tensile strength will drop sharply, and from 3 to 6%, it will decrease at a slower rate. The reason for this decrease is that nanoclay, like ceramic materials, absorbs heat and acts as a heat insulating material; hence less heat reaches the polymer and less melting takes place which causes less penetration at the joint, and consequently lower weld strength. It is therefore concluded that increase in clay content reduces weld strength. The SEM images shown in Figures 7(a) and 7(b) also indicate that rougher surface which is due to less clay content leads to a higher weld strength compared to the one having a smooth surface with 3% clay content.

TABLE 3. Test validation results

Row	C (%)	ω (rev/min)	v (mm/min)	T (ºC)	Tensile Strength (MPa)	Error (%)
1	0	800	10	75	Real:12.87, Predicted:13.50	4.8
2	3	1200	15	50	Real:9.24, Predicted:8.72	5.6
3	6	1600	20	100	Real:8.83, Predicted:8.99	3.3

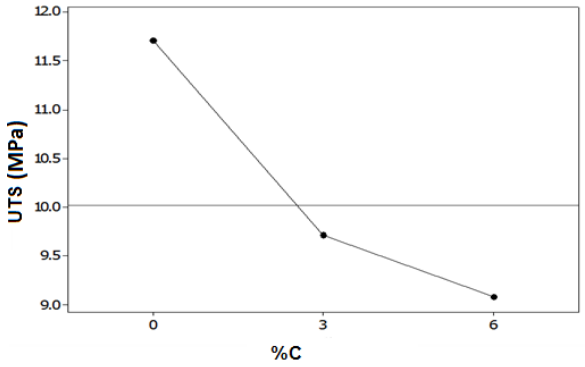

Figure 6. The effect of clay content on weld tensile strength

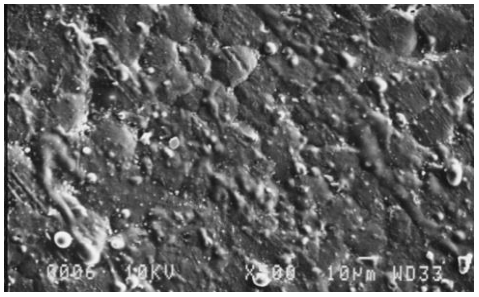

(a)

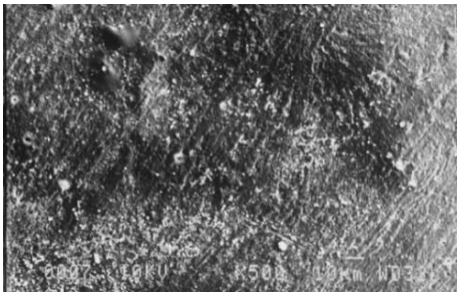

(b)

Figure 7. Weld surface, a) without clay, b) with 3% clay

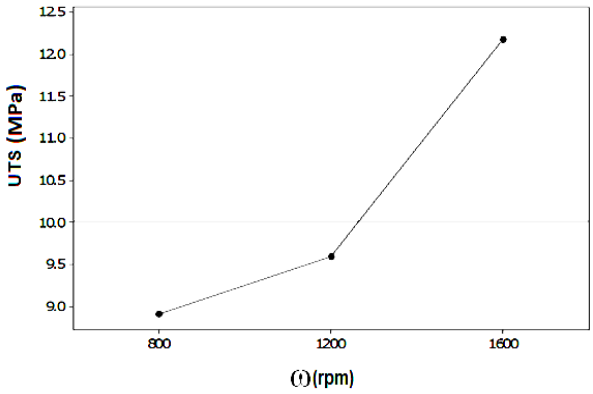

Figure 8. The effect of rotational velocity on weld tensile strength

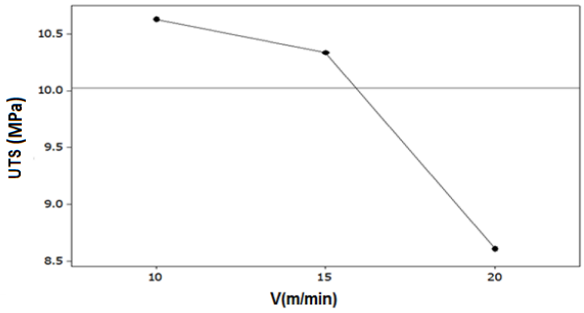

Figure 9. Effect of linear velocity on tensile strength

3. 4. 2. The Effect of Rotational Velocity on Tensile Strength As shown in Figure 8, with increasing rotational velocity from 800 to 1200 rpm, the tensile strength increased slightly, but increasing it from 1200 to 1600 rpm led to more increase in tensile strength. With increasing the rotational speed of the pin, the local temperature of material would rise. This can be attributed to low thermal conductivity of polymeric material, which leads to heat concentration at the weld nugget. Hence, more molten material would be present at the joint line that leads to more penetration as well as improved weld performance with a consequence of increase in weld tensile strength.

3. 4. 3. The Effect of Linear Velocity on Weld Tensile Strength Figure 9 shows the effect of linear velocity on weld tensile strength. Tensile strength remains nearly unchanged for linear velocities from 10 to 15 mm/min, but decreases from 15 to 20 mm/min. The reason for this decrease in strength at high linear velocities is the lack of enough time for pin to produce the required heat for welding, which leads to a decrease in strength. As a result, with a decrease in linear velocity, the strength of the weld would increase.

3. 4. 4. The Effect of Tool Temperature on Tensile Strength The effect of tool temperature on tensile strength of the weld is shown in Figure 10. It is observed that with an increase in temperature from 50 to 75°C, the tensile strength of the weld would increase and with an increase from 75 to 100 °C it would decrease. This figure indicates that an optimal temperature of 75 °C exists which can yield maximum weld strength. In Figure 11, due to the low temperature, the materials at the joint did not penetrate into each other sufficiently. As a result, the weld is of less strength. At high temperature, the weld strength is again low. This may be attributed to the tendency of the weld to partially evaporate at high temperatures particularly if the frictional heat is high. Figure 12 shows an inadequate weld due to evaporation with its SEM image taken from the fractured surface.

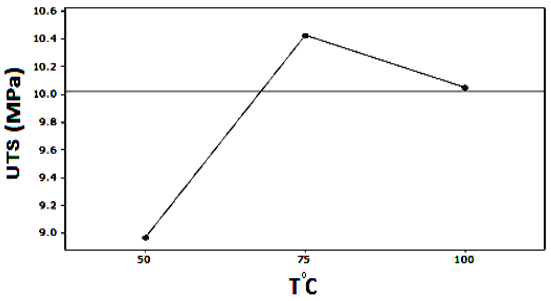

Figure 10. The effect of tool temperature on tensile strength

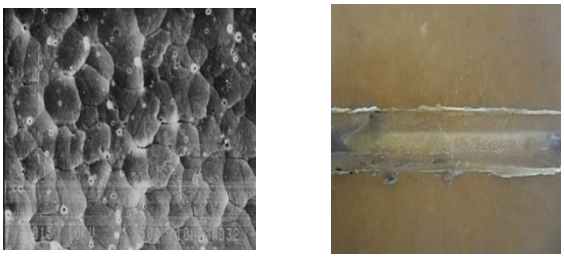

Figure 11. Low strength and poor joint at low tool temperature

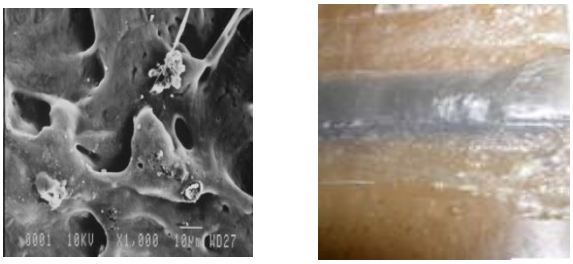

Figure 12. An inadequate weld with its SEM image

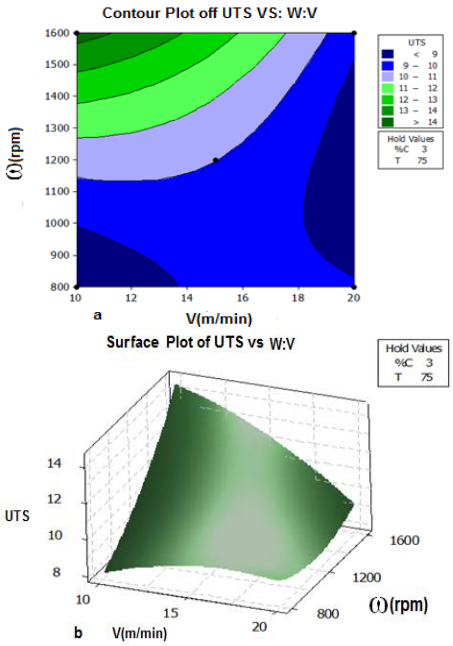

Figure 13. Interaction effect of linear velocity and rotational speed on weld strength; a) contour plot b) surface plot

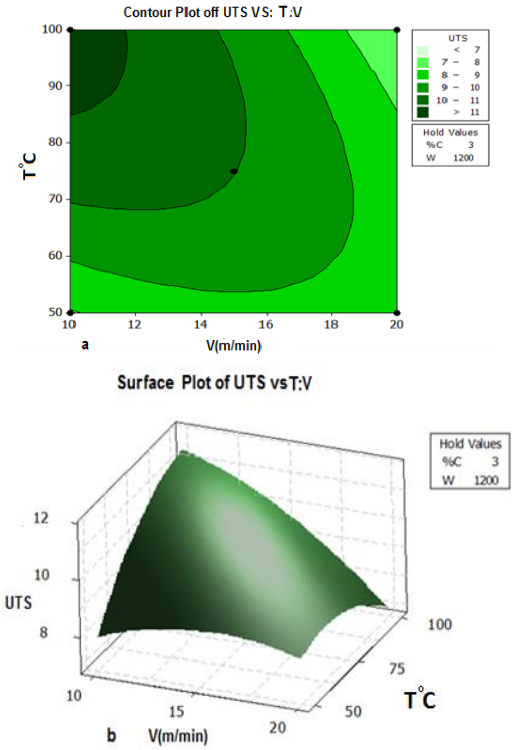

Figure 14. Interaction effect of tool temperature and rotational speed on weld strength; a) contour plot b) surface plot

3. 4. 5. Optimal Areas with Contour and Surface Plots Contour and surface plots show how a response variable depends on two or several factors. After investigating model adequacy, the regression equation is used to plot contour and surface diagrams for the response. Since the interactions are effective (in the process), their contour and surface plots are shown in Figures 13 and 14. These plots are obtained from regression model through Minitab® 16 software for ultimate tensile strength. Figure 13 shows the effect of interaction of linear speed (V) and rotational speed (ω) on weld strength. According to Figures 13 (a) and (b), the highest value of tensile strength was obtained from higher left corner of the contour and surface plots, i.e. when ω was at its highest and V at its lowest value. The reason for this behaviour may be attributed to more stirring at the weld nugget due to high rotational velocity and low linear speed. Also, the minimum tensile strength can be obtained when proper combinations of linear speed (e.g. 10 – 12 mm/min) and rotational speed of (e.g. 800 -1000 rpm) are selected. According to Figure 14, the highest value of tensile strength is obtainable from upper left corner of the plot, i.e. when tool temperature was at its highest and linear speed at its lowest value. The increase in tool temperature (preheating) at the weld nugget may

improve stirring action and hence the tensile strength would rise up. According to this figure, the optimum weld strength can be obtained when selecting a proper combination of the linear speed at 10 - 12 mm/min and tool temperature at 85 -100°C. Also, with the linear speed of 18-20 mm/min when tool temperature was 85-100°C, the minimum weld strength was obtained.

4. CONCLUSION

On the basis of the research conducted on FSW of PP/EPDM/clay nanocomposites, it is concluded that:

1. All the input parameters are significant and the obtained equation for prediction of weld tensile strength is acceptable.
2. More clay content in the nanocomposite causes rougher fracture surface and higher strength.
3. With increasing rotational velocity, weld strength would increase.
4. With increase in linear velocity and clay content in the nanocomposite, the weld strength decreases.
5. Increasing the temperature from 50 to 75°C increases the weld tensile strength but from 75 to 100°C the weld strength decreases.
6. In samples with 0, 3 and 6% clay content, the weld tensile strength equals to 94, 80 and 60% of the respective base material.

5. REFERENCES

1. Khosrokhavar, R., Naderi, G., Bakhshandeh, G.R. and Ghoreishy, M.H.R., "Effect of processing parameters on pp/epdm/organoclay nanocomposites using taguchi analysis method", ***Iran Polym Journal***, Vol. 20, (2011), 41-53.
2. Nikoi, R., Sheikhi, M. and Arab, N.B.M., "Experimental analysis of effects of ultrasonic welding on weld strength of polypropylene composite samples", ***International Journal of Engineering-Transactions C: Aspects***, Vol. 28, No. 3, (2014), 447-453.
3. Khalili, R. and Eisazadeh, H., "Preparation and characterization of polyaniline/sb2o3 nanocomposite and its application for removal of pb (ii) from aqueous media", ***International Journal of Engineering-Transactions B: Applications***, Vol. 27, No. 2, (2013), 239-246.
4. Shafiei, S. and Salahi, E., "Effect of combination on properties of cu-ag nanocomposites synthesized by heat treatment", ***International Journal of Engineering-Transactions B: Applications***, Vol. 23, No. 3&4, (2010), 209-216.
5. Heydari, A., Alemzadeh, I. and Vossoughi, M., "Influence of glycerol and clay contents on biodegradability of corn starch nanocomposites", ***International Journal of Engineering-Transactions B: Applications***, Vol. 27, No. 2, (2013), 203-212.
6. Babu, S., Elangovan, K., Balasubramanian, V. and Balasubramanian, M., "Optimizing friction stir welding parameters to maximize tensile strength of aa2219 aluminum alloy joints", ***Metals and Materials International***, Vol. 15, No. 2, (2009), 321-330.
7. Zhang, Z. and Zhang, H., "Numerical studies on the effect of transverse speed in friction stir welding", ***Materials & Design***, Vol. 30, No. 3, (2009), 900-907.
8. Nakhaei, M., Arab, N.M. and Naderi, G., "Application of response surface methodology for weld strength prediction in laser welding of polypropylene/clay nanocomposite", ***Iranian Polymer Journal***, Vol. 22, No. 5, (2013), 351-360.
9. Su, J.-Q., Nelson, T., Mishra, R. and Mahoney, M., "Microstructural investigation of friction stir welded 7050-t651 aluminium", ***Acta Materialia***, Vol. 51, No. 3, (2003), 713-729.
10. Ahmadi, H., Arab, N.M., Ghasemi, F.A. and Farsani, R.E., "Influence of pin profile on quality of friction stir lap welds in carbon fiber reinforced polypropylene composite", ***International Journal of Mechanics and Applications***, Vol. 2, No. 3, (2012), 24-28.
11. Bagheri, A., Azdast, T. and Doniavi, A., "An experimental study on mechanical properties of friction stir welded abs sheets", ***Materials & Design***, Vol. 43, (2013), 402-409.
12. Yousefpour, A., Hojjati, M. and Immarigeon, J.-P., "Fusion bonding/welding of thermoplastic composites", ***Journal of Thermoplastic Composite Materials***, Vol. 17, No. 4, (2004), 303-341.
13. Kiss, Z. and Czigany, T., "Microscopic analysis of the morphology of seams in friction stir welded polypropylene", ***Express Polym Lett***, Vol. 6, No. 1, (2012), 54-62.
14. Payganeh, G., Arab, N.M., Asl, Y.D., Ghasemi, F. and Boroujeni, M.S., "Effects of friction stir welding process parameters on appearance and strength of polypropylene composite welds", ***International Journal of Physics Science***, Vol. 6, No. 19, (2011), 4595-4601.
15. Pirizadeh, M., Azdast, T., Ahmadi, S.R., Shishavan, S.M. and Bagheri, A., "Friction stir welding of thermoplastics using a newly designed tool", ***Materials & Design***, Vol. 54, (2014), 342-347.
16. Azarsa, E. and Mostafapour, A., "On the feasibility of producing polymer–metal composites via novel variant of friction stir processing", ***Journal of Manufacturing Processes***, Vol. 15, No. 4, (2013), 682-688.
17. Mendes, N., Loureiro, A., Martins, C., Neto, P. and Pires, J., "Effect of friction stir welding parameters on morphology and strength of acrylonitrile butadiene styrene plate welds", ***Materials & Design***, Vol. 58, (2014), 457-464.
18. Hosseinpour, M., Najafpour, G., Younesi, H., Khorrami, M. and Vaseghi, Z., "Lipase production in solid state fermentation using aspergillus niger: Response surface methodology", ***International Journal of Engineering***, Vol. 25, No. 3, (2012), 151-159.

APPENDIX

A) Design matrix and the collected experimental data

Row	Test no	Clay nanoparticles	Rotational velocity (rpm)	Linear velocity (mm/min)	Temperature (°C)	Tensile strength (MPa)
1	23	3	800	15	100	9.48
2	4	6	1600	15	75	12.86
3	20	6	1200	20	75	8.11
4	26	3	1200	15	75	9.98
5	14	3	1600	10	75	13.75
6	21	3	800	15	50	7.84
7	19	0	1200	20	75	9.19
8	5	3	1200	10	50	7.55
9	12	6	1200	15	100	9.11
10	10	6	1200	15	50	7.05
11	3	0	1600	15	75	14.04
12	17	0	1200	10	75	13.39
13	1	0	800	15	75	10.98
14	25	3	1200	15	75	10.20
15	22	3	1600	15	50	11.34
16	15	3	800	20	75	9.52
17	13	3	800	10	75	8.17
18	27	3	1200	15	75	9.84
19	9	0	1200	15	50	11.42
20	7	3	1200	10	100	11.05
21	11	0	1200	15	100	11.26
22	24	3	1600	15	100	12.10
23	2	6	800	15	75	7.52
24	16	3	1600	20	75	8.98
25	6	3	1200	20	50	8.62
26	18	6	1200	10	75	9.86
27	8	3	1200	20	100	7.29

B) ANOVA test for the weld tensile strength

Source	Seq SS	DF	Adj MS	F - value	P - value
Regression	102.7	14	7.34	22.62	0
Linear	68.2	4	17.05	52.54	0
%clay	20.7	1	20.72	63.84	0
Rotational velocity	21.8	1	31.8	98.22	0
Linear velocity	12.1	1	12.1	37.34	0
Temperature	3.4	1	3.48	10.75	0.01
Square	15.1	1	3.78	11.66	0
C*C	3.1	1	1.73	5.35	0.04
ω* ω	8.2	1	3.36	10.36	0.01
V*V	0.68	1	1.87	5.78	0.03
T*T	3.1	1	3.117	9.60	0.01
Interaction	19.4	6	3.237	9.97	0
C*ω	1.30	1	1.292	4	0.07
C*V	1.5	1	1.500	4.62	0.05
C*T	1.23	1	1.232	3.80	0.08
ω *V	9.3	1	9.363	28.84	0
ω *T	0.19	1	0.193	0.60	0.5
V*T	5.8	1	5.832	17.97	0.01
Residual Error	3.8	12	0.324		
Lack-of-Fit	3.8	10	0.383	13.60	0.01
Pure	0.05	2	0.028		
Total	106.6	26			
R^2= 96.35%		**R^2_{Pred}=79.15%**			

Investigation on Tensile Strength of Friction Stir Welded Joints in PP/EPDM/Clay Nanocomposites

G. R. Rezaei, N. Bani Mostafa Arab

Faculty of Mechanical Engineering, Shahid Rajaee Teacher Training University, Tehran, Iran

P A P E R I N F O

Paper history:
Received 25 May 2015
Received in revised form 12 July 2015
Accepted 30 July 2015

Keywords:
Nanocomposite
Friction Stir Welding
Clay
Response Surface Method
Tensile Strength

چکیده

نانوکامپوزیت‌های پایه پلیمری به دلیل مقاومت خوب در برابر خوردگی، خواص مکانیکی مناسب و کم هزینه بودن به طور گسترده در فناوری‌های مدرن استفاده می‌شوند. به دلیل رشد فزاینده استفاده از این نانوکامپوزیت‌ها، اتصال آنها با استفاده از فرایندهای جوشکاری به نظر اجتناب ناپذیر می‌آید. دراین مقاله، صفحات ۵ میلی‌متری نانوکامپوزیتی که شامل پلی پروپیلن ، اتیلن پلی پروپیلن دی ان مونومرو مقادیر متفاوت ۰، ۳ و ٦ در صد نانو ذرات خاک رس می باشند با استفاده از یک ابزار داغ جدید درفرایند جوشکاری اصطکاکی اغتشاشی به صورت لب به لب جوشکاری شدند. برای طراحی آزمایشات از روش سطح پاسخ استفاده شد تا تاثیر پارامترهای فرآیند مانند سرعت چرخشی ابزار، سرعت خطی جوشکاری، دمای شانه ابزار و درصد ذرات خاک رس بر استحکام کششی جوش تعیین گردد. نتایج تحقیق نشان داد که اگرچه افزایش مقدار خاک رس در مواد پایه استحکام کششی این مواد را افزایش می دهد، اما باعث کاهش استحکام کششی جوش آنها می‌شود به طوری که در نمونه‌های با ۰، ۳ و ٦ در صد خاک رس، استحکام کششی جوش به ترتیب برابر ۹٤، ۸۰ و ٦۱ درصد مواد پایه می‌گردد.

***doi**: 10.5829/idosi.ije.2015.28.09c.17*